Physica C 506 (2014) 146–150

Contents lists available at ScienceDirect

Physica C

journal homepage: www.elsevier.com/locate/physc

Tower as magnetic antipinning core in a small superconducting sample

J. Barba-Ortega [a,*], Miryam R. Joya [a], Edson Sardella [b,c]

[a] Departamento de Física, Universidad Nacional de Colombia, Bogotá, Colombia
[b] UNESP – Universidade Estadual Paulista, Departamento de Física, Caixa Postal 473, Bauru, SP, Brazil
[c] UNESP – Universidade Estadual Paulista, IPMet – Instituto de Pesquisas Meteorológicas, CEP 17048-699 Bauru, SP, Brazil

ARTICLE INFO

Article history:
Received 9 April 2014
Accepted 17 June 2014
Available online 26 June 2014

Keywords:
Vortex
Ginzburg–Landau
Mesoscopic
Pillars

ABSTRACT

Using the nonlinear Ginzburg–Landau equations we study the vortex configurations in a superconducting square with a central square pillar in the presence of a uniform applied magnetic field. The presence of the pillar changes the vortex structure in the superconducting sample considerably. We calculate magnetization, magnetic induction, supercurrent and vorticity, which show different vortex configurations as a function of magnetic field.

1. Introduction

Usually the antipinning/pinning centers, the geometry/size of the sample and the energy surface barrier are considered to be competing effects that alternatively control the magnetic response in the vortex state. The superconducting properties of samples with engineered manufactured barriers/pillars have attracted over the past decade [1,2]. Motivated by technological advances, superconductors with different types of defects revealed a diversity of new phenomena. The possibility of controlling the vortex dynamics and the critical fields has made from mesoscopics superconductors one of the favorite experimental and theoretical systems for studies of the physics of condensed matter [3–7]. It was observed that due to the influence of vortex shell structures in thin Nb samples, a transition from Abrikosov-like vortex lattice to vortex shell structures take place at interstitial sites. Also, when the pillars are placed closer, the vortex patterns depend on their density and the pillar size [2]. In previous works we studied the effects associated to the pinning force of both a point-like and circular defect on the vortex configuration, thermodynamical properties and the vortex entry and expulsion fields in a very thin disk. We found that due to vortex-defect attraction (repulsion), the vortices always (never) are found to be sitting on the defect position. In addition, for the circular defect, we found a vortex–antivortex state at zero magnetic field [8] and non-conventional vortex configurations [9]. Now, in continuation of previous work of vortex-defect interaction, we have gone further by calculating the magnetization, free energy, vorticity and Cooper pair density for a square sample of area $S = 144\xi^2$, with a central square pillar of cross section area T^2, for $T/\xi = 2, 4, 6, 8$, where ξ is the coherence length.

2. Theoretical formalism

The general form of the time dependent Ginzburg–Landau equations are [10–12]:

$$\frac{\partial \psi}{\partial t} = -(-i\nabla - \mathbf{A})^2\psi + \psi(1 - |\psi|^2), \quad (1)$$

$$\frac{\partial \mathbf{A}}{\partial t} = \mathrm{Re}\left[\bar{\psi}(-i\nabla - \mathbf{A})\psi\right] - \kappa^2\nabla \times \nabla \times A. \quad (2)$$

In Eqs. (1) and (2) dimensionless units were introduced as follows: ψ is the order parameter in units of $\psi_\infty = \sqrt{-\alpha/\beta}$, where α and β are two phenomenological constants; lengths in units of the coherence length ξ; time in units of $t_0 = \pi\hbar/8K_BT_c$; $\mathbf{A}$ in units of $H_{c2}\xi$, where H_{c2} is the second (upper) critical field for bulk superconductors. For a very thin film of variable thickness, Eq. (1) can be rewritten as [13,14]:

$$\frac{\partial \psi}{\partial t} = -\frac{1}{g}(-i\nabla - \mathbf{A}) \cdot g(-i\nabla - \mathbf{A})\psi + \psi(1 - |\psi|^2), \quad (3)$$

$$\frac{\partial \mathbf{A}}{\partial t} = \mathrm{Re}\left[\bar{\psi}(-i\nabla - \mathbf{A})\psi\right] - \kappa^2\nabla \times \nabla \times A, \quad (4)$$

where now all the quantities depend only on the coordinates (x, y) and $g = g(x, y)$ is just a function which describes the thickness of the

* Corresponding author. Tel.: +57 3173141682; fax: +57 3165000 13082.
E-mail address: jjbarbao@unal.edu.co (J. Barba-Ortega).

http://dx.doi.org/10.1016/j.physc.2014.06.007
0921-4534/

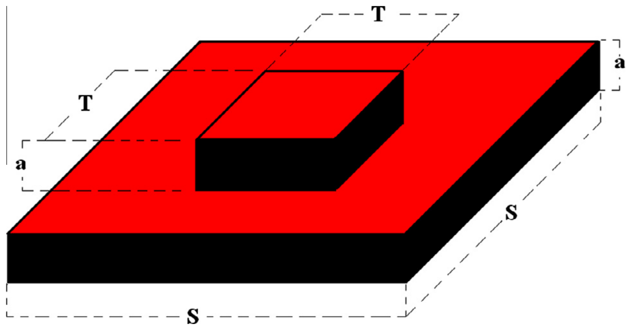

Fig. 1. Illustration of a square superconductor with a pillar on the top.

sample [15]. We consider $g(x,y) = 1$ everywhere, except at the pillar position in the sample, where $g(x,y)$ is slightly larger than one. The passage from Eqs. (1) and (2) to (3) and (4) requires an average of the original equations along the z direction by considering a film of thickness $c \ll \xi$. We simulate a mesoscopic superconducting sample of area $S^2 = 144\xi^2$ with a central pillar of area T^2, for $T/\xi = 2,\ 4,\ 6,\ 8$. The height of the pillar and square are $a = 0.5\xi$. In Fig. 1 we illustrate the schematic view of square superconductor with a pillar on the top of it.

3. Results and discussion

Fig. 2 shows the magnetization $4\pi M$ (up) and vorticity N (down) as functions of the applied magnetic field, both on the left column, when H_e is increasing, and decreasing (right column) for $T/\xi(0) = 2,\ 4,\ 6,\ 8$. As can be seen from the panels of Fig. 2, the upper and lower critical fields H_2 and H_1 are approximately independent of the size of small defects in the sample; we have $H_1 = 0.620$ for $T/\xi = 2,\ 4,\ 6$, but $H_1 = 0.682$ for $T/\xi = 8$. In other words, both the filed barrier for the first penetration and the applied field sufficient to destroy superconductivity do not alter significantly with variation of the pillar size. Furthermore, it is clearly seen that, for all cases the upper thermodynamical critical field H_2 occurs at the same value $H_2 = 1.8$.

Another interesting characteristic in the downward branch of the magnetic field, is that the vortex expulsion fields are different as T/ξ varies. The final vortex transitions when the magnetic field is decreasing occur at different values of H_p when the magnetic field is decreasing: $N = 4 \rightarrow 0$ occurs at $H_p = 0.460$ for $T = 8\xi$, $H_p = 0.340$ for $T = 6\xi$, at $H_p = 0.139$ for $d = 4\xi$ and finally a vortex transition $N = 2 \rightarrow 0$ occurs at $H_p = 0.072$ for $T = 2\xi$. This is consistent with the fact that the more efficient the pillar acts as an anti-pinning as we have argued above. In Fig. 3 we plot the Cooper pairs density $|\psi|^2$ (a), the current density $\mathbf{J}_s = \mathrm{Re}[\bar{\psi}(-i\nabla - \mathbf{A})\psi]$ (b), the order parameter phase $\Delta\phi$ (c), and the magnetic induction $\mathbf{h}$ (d), for $H_e = 0.724$ in the increasing branch of the magnetic field and several values of T/ξ in the upper panel of the figure, and decreasing branch of the applied filed in the lower panel of the same figure. We can observe in the order parameter density plot that for $d = 2\xi(0)$, there are $N = 4$ vortices into the sample, one in each corner of the pillar and no vortices in the pillar. For larger values of T, the same four vortices nucleate on the square, but they are placed on opposite sides of the pillar. It

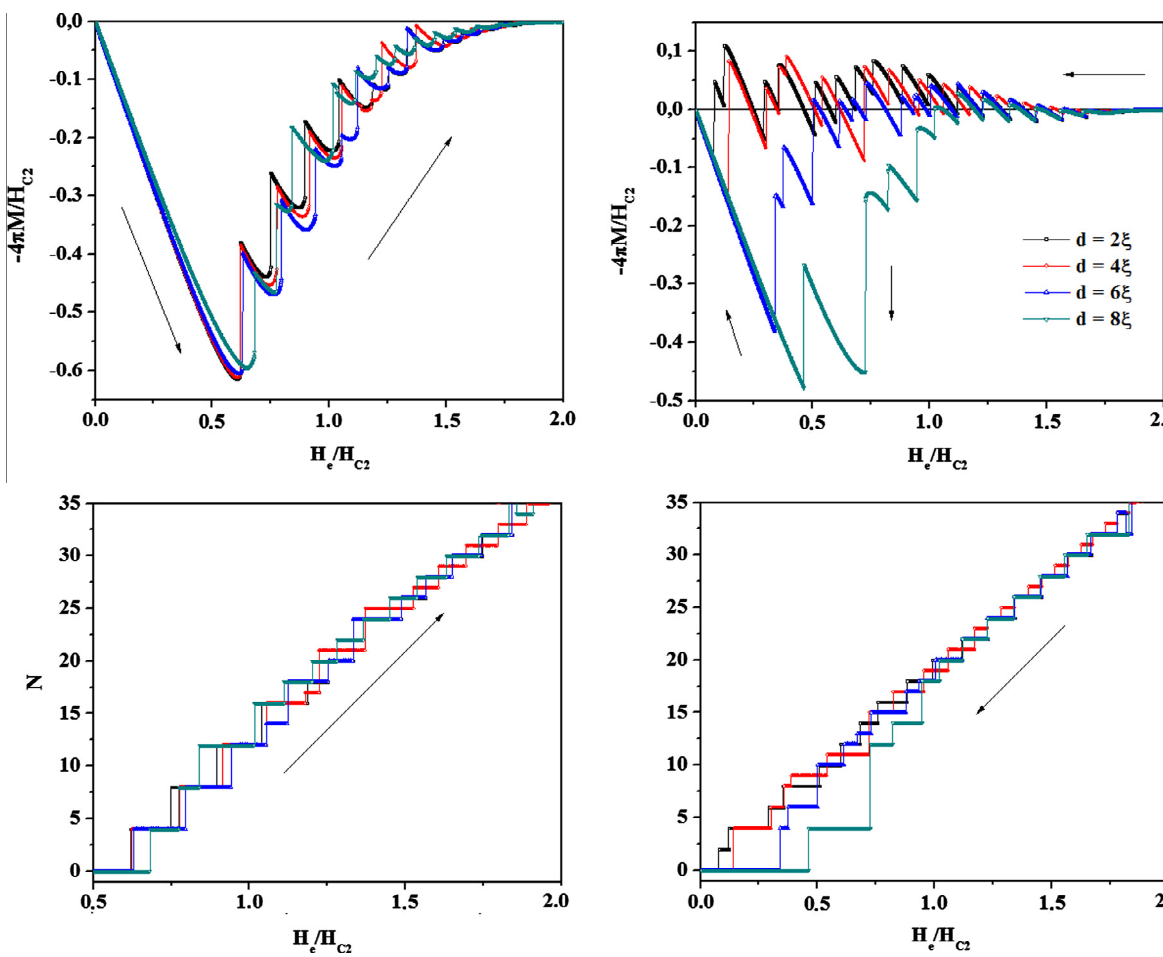

Fig. 2. Magnetization $4\pi M$ (up) and vorticity N (down) as functions of the applied magnetic field when it is increasing (left) and decreasing (right) for several values of T/ξ.